Measurement, Analysis, and Denoising of Directional Room Impulse Responses in Complex Spaces

Pierre Massé, Thibaut Carpentier, Olivier Warusfel, Markus Noisternig

MEASUREMENT, ANALYSIS, AND DENOISING OF DIRECTIONAL ROOM IMPULSE RESPONSES IN COMPLEX SPACES

Pierre Massé[1] **Thibaut Carpentier**[1] **Olivier Warusfel**[1] **Markus Noisternig**[1]
[1] Acoustic and Cognitive Spaces group
STMS, Sorbonne Université, Ircam, CNRS 75004 Paris, France
pierre.masse@ircam.fr

ABSTRACT

The use of directional room impulse responses (DRIR) measured with spherical microphone arrays (SMA) has become widespread in the reproduction of spatial reverberation effects on surround-sound systems through multichannel convolution. However, the measurement of such DRIRs in "real-world" conditions is inevitably subject to several risk factors, including the presence of a non-decaying noise floor that can produce an "infinite reverberation" effect when convolved with an input sound. Recent work has focused on model-based techniques for removing this noise floor by replacing it with a re-synthesized prolongation of the measured reverberation tail, which has concurrently led to the development of a framework for the spatial analysis of reverberation properties.

We present here a comprehensive evaluation of the proposed techniques through their application to DRIRs measured in particularly complex spaces, including spatially anisotropic late reverberation tails as well as multiple-slope decays characteristic of coupled-volume configurations. Following a brief review of the theoretical underpinnings of the reverberation tail re-synthesis denoising procedure, the measurement, treatment, analysis, and subsequent denoising of these DRIRs are each detailed and assessed with quantitative metrics. Finally, a discussion of the anisotropic, direction-dependent analysis results obtained is included as the basis for a wider research question on the acoustical considerations behind a stochastic reverberation model allowing for spatial variations.

1. INTRODUCTION

The increasingly widespread use of multi-channel DRIR convolution for recreating spatialized reverberation effects has generated a large field of research onto itself, from SMA signal processing to room acoustics modeling to the human perception of spatialized sound. In order for DRIRs measured in real-world conditions to be used in any subsequent applications, most notably those involving reproduction over loudspeaker arrays such as Higher-Order Ambisonics (HOA) "domes", it is imperative to both detect and compensate the inevitable non-decaying measurement noise floor. Failure to do so results in the noise floor being convolved with the input sound along with the "true" decaying impulse response, which can produce an audible "infinite reverberation" artefact.

The idea of replacing this noise floor with a re-synthesized extrapolation of the DRIR's exponentially-decaying reverberation tail was first proposed in a monophonic context by Jot *et al.* [1], building on the work of Schroeder [2], Moorer [3], and Polack [4]. It was extended to DRIRs first by Carpentier *et al.* [5] and Noisternig *et al.* [6], before finally being formalized in the spherical harmonic (SH) domain by Massé *et al.* in the case of isotropic or "diffuse" late fields [7] and through plane-wave decomposition (PWD) for anisotropic cases [8].

Here we wish to present various applications of the analysis-synthesis framework that has resulted from this chain of research. The selected examples have been chosen to cover a wide range of spaces, from more traditional enclosed rooms where diffuse-field conditions are easily verified, to highly anisotropic semi-open spaces and coupled-volume configurations. Evaluating the results obtained from these examples provides a thorough assessment of the framework's advantages and limitations.

1.1 Related Work

Preliminary investigations into human capacity for the perception of anisotropy in the spatial power distribution of incoherent late reverberation were carried out by Romblom *et al.* [9]. Complementary work on objective directional analysis metrics by Berzborn and Vorländer [10] and Alary *et al.* [11] has provided a framework for detailing the spatial power distribution in the late reverberation tails of measured DRIRs. Finally, Nolan *et al.* [12] have proposed a method for quantifying the degree of isotropy in a sound field through a single measure similar to Ahonen and Pulkki's pseudo-intensity vector diffuseness [13].

2. SPATIAL REVERBERATION ANALYSIS

The analysis framework used in the present work aims to construct a model of the exponentially decaying late reverberation energy decay envelope by acting on an appropriate spatial representation of the DRIR. In cases where the decaying spatial power distribution is determined to remain isotropic (or "close enough") throughout, analysis and re-synthesis can be performed directly in the SH domain [7]. Conversely, if a large degree of anisotropy is achieved at any point in the reverberation tail, re-synthesis based on the analyzed power distribution must be direction-dependent (since arbitrarily anisotropic power distributions cannot be

represented in the SH domain) and therefore the framework makes use of a PWD steered around the sphere [8].

2.1 Plane Wave Decomposition

The number of directions that the SH representation can be decomposed onto is limited by the total number of SH components, since the resulting signals must be linearly independent in order to preserve the late reverberation field's spatial incoherence [8]. In fact, in order to re-encode to the SH domain after the direction-dependent analysis and treatment, the number of PWD directions must be exactly equal to the number of SH components. For 4$^{\text{th}}$-order SH signals (25 components), a Fliege-type grid [14] was found to best preserve spatial incoherence while garanteeing an even (low variance) total directivity over the sphere [8]. We note that in such a discretized and order-truncated context, the PWD formalism is equivalent to a (natural) beamformer, in particular a hypercardioid in the 4$^{\text{th}}$-order case.

The direction of arrival (DoA) of the direct sound is used as a reference direction to rotate the Fliege set of directions such that one beam is facing the DoA. The direct sound's temporal position is first estimated using the measured field's spatial coherence properties: assuming relatively low harmonic distortion, the direct sound should be responsible for the first significant increase in spatial coherence during the course of the DRIR. In practice, this spatial coherence is calculated as a measure of incoherence between directional beams in an analogous manner to the COMEDIE diffuseness measure in the SH domain [15], but using a power-normalized covariance function [8].

The detected initial coherence peak represents a certain time frame within which the first match for an ideal impulsive signal can be found on the omnidirectional (zeroth-order) SH component. Following an initial "blind" PWD (on a non-rotated grid), the total energy from the samples corresponding to the detected impulse can be interpolated over the sphere, e.g. by spherical cubic Hermite interpolation [16], in order to find the energy peak of the direct sound and thus identify its DoA. The Fliege grid can then be rotated towards this direction, the PWD re-applied, and the procedure re-iterated until the DoA detection converges. It should be noted that other DoA detection methods can also be used here, including directly exploiting the first-order SH signals [17], or through subspace methods such as multiple signal classification (MUSIC) or estimation of signal parameters through rotational invariant techniques (ESPRIT) [18]. Such techniques may help avoid inaccuracies due to rapidly-arriving early reflections, but can also be subject to angular ambiguities in special cases.

2.2 Mixing Time Estimation

"Late reverberation" traditionally refers to the time-frequency region in a room impulse response where the classic exponentially-decaying stochastic model for a room's acoustic response to a steady-state excitation become valid [2] [3] [4]. This validity domain is defined by a lower frequency bound known as the Schroeder frequency, which corresponds to a modal density condition, and a lower time bound known as the "mixing time", which corresponds to an echo density condition.

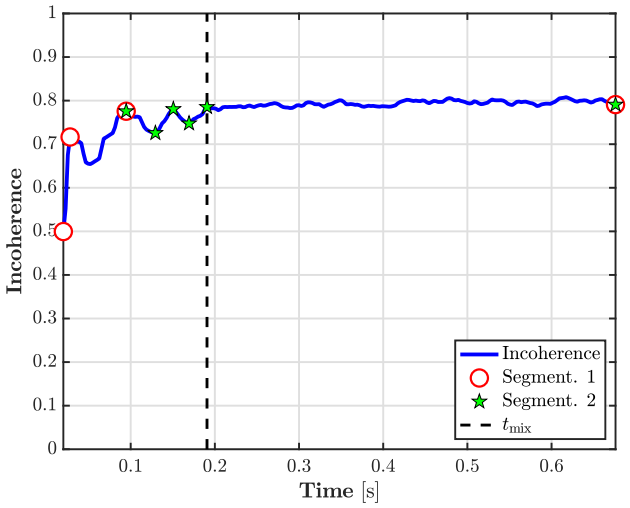

Figure 1. Mixing time (t_{mix}, black dashed line) estimation on the spatial incoherence profile (blue solid line) of a DRIR measured at the Lille opera house, using a two-fold RDP segmentation (red circles and green stars).

It follows that in the validity domain, the acoustic field can theoretically be described as the superposition of an "infinite" number of statistically independent plane waves [19]. This in turn implies that, when adding a spatial dimension to the stochastic model, the late reverberation field should be spatially or directionally incoherent (from the point of view of an SMA).

The sound field's spatial coherence properties can thus also be exploited in order to estimate the mixing time [8]. Evaluating the spatial incoherence measure over the course of the DRIR gives an "incoherence profile" which can then be segmented using an adaptive Ramer-Douglas-Peucker (RDP) algorithm [20], which essentially aims to fit the curve using segment-wise linear regressions (red circles, Fig. 1). This enables the detection of the longest, most "stable" (smallest slope) segment of the incoherence curve, corresponding to the late reverberation tail. When this is applied to a noisy measurement, the noise floor limiting time should be first estimated (see Sec. 2.4 below) and the incoherence profile truncated accordingly in order to avoid detecting the noise floor itself as the mixing time.

The identified segment can be further re-segmented (green stars, Fig. 1) in order to detect and avoid any irregularities near its onset due to late-arriving coherent echoes. This is achieved here by choosing the mixing time as the start of the first sub-segment whose "score" (the geometric mean of the segment's length and the inverse of its slope) is above the mean over all sub-segments (those obtained by re-segmenting the first detected segment).

2.3 Isotropy Analysis by Energy Decay Deviation

The isotropy of the late reverberation is evaluated using a measure of energy decay deviation (EDD) [11], which is defined as:

$$\mathrm{EDD}(\Omega_d, t) = \mathrm{EDC}_{\mathrm{dB}}(\Omega_d, t) - \overline{\mathrm{EDC}}_{\mathrm{dB}}(t), \quad (1)$$

where $\mathrm{EDC}_{\mathrm{dB}}(\Omega_d, t)$ refers to the dB-scale Schroeder reverse-integrated energy decay curve (EDC) of the signal at each PWD direction Ω_d, and $\overline{\mathrm{EDC}}_{\mathrm{dB}}(t)$ represents the average over the set of all PWD directions. The EDD therefore represents the spatial deviation from the mean power at a given time step. From this, a simple measure of the degree of anisotropy can be obtained by averaging the "dynamic range" of the EDD,

$$\Delta\mathrm{EDD}(t) = \max_{\Omega_d}[\mathrm{EDD}(\Omega_d, t)] - \min_{\Omega_d}[\mathrm{EDD}(\Omega_d, t)], \quad (2)$$

over the length of the late reverberation tail.

Note that the EDD is only evaluated over the length of the late reverberation, i.e. from the mixing time to the moment the noise floor is reached; both of these values must therefore first be estimated. Furthermore, to avoid the inherent limitations of SH-encoded SMA measurements, namely low-frequency omnidirectionality due to the application of regularized rigid sphere scattering correction filters [21] and high-frequency spatial aliasing [22], the EDCs are calculated on signals filtered to within five octaves below the SMA's spatial aliasing limit.

2.4 Late Reverberation Modeling

The frequency-dependent energy decay envelope parameters of the late reverberation are extracted from the energy decay relief (EDR), a time-frequency extension of the Schroeder EDC [1]. This gives a decay curve at each frequency bin which can be analyzed in three main steps, which are further detailed in Massé *et al.* [7]. Briefly, the curve is first segmented, once again using an adaptive RDP algorithm [20], which helps identify the different sections (early reflections, exponential decay, and noise floor); the noise floor is then detected by fitting the theoretical dB-scale profile of a reverse-integrated constant-power noise; finally, the exponential decay model can be fitted to the curve segment(s) between the early, non-exponential reflection regimes and the noise floor.

This analysis enables the extraction of several important model parameters: the decay rate, usually represented as the 60 dB reverberation time (T_{60}), the initial power spectrum of the late reverberation (P_0, not to be confused with the power spectrum of the direct sound), and the noise floor limiting time (t_{lim}, i.e. the moment the decay envelope stops being exponential due to encountering the non-decaying measurement noise floor).

2.5 Denoising by Tail Re-Synthesis

An important application of the analysis and modeling techniques described above is in the compensation of the non-decaying measurement noise floor. As mentioned in Sec. 1, this can be done by replacing it with a re-synthesized prolongation of the late reverberation tail, using a zero-mean Gaussian noise signal subjected to an exponentially decaying envelope parameterized by the DRIR analysis. In the case of isotropic DRIRs, this can be done directly in the SH domain [7], and in the anisotropic case the same process must be applied in a direction-dependent manner [8] (i.e. on the steered PWD signals). In either case, the use of a zero-mean Gaussian noise signal ensures that the resulting sound field is spatially incoherent, as required by the stochastic model.

More precisely, for each frequency bin of each component or directional signal, the time frames from t_{lim} onwards are replaced by the corresponding frequency bin of the zero-mean Gaussian noise, to which the prolonged energy decay envelope is then applied as generated by the extracted model parameter values. The DRIRs presented in this work will each have been denoised in this manner.

3. MEASURED SPACES

In order to provide a qualitative context to the results presented in Sec. 4, the various measurements to be evaluated are briefly described below. All DRIRs were measured using a 32-capsule mh acoustics Eigenmike® and then encoded to the 4th-order SH domain before being analyzed through a PWD steered over a 25-point Fliege grid following the procedure described above (Sec. 2).

3.1 Enclosed Spaces

A measurement from a space presenting highly isotropic late reverberation with a single exponential decay was chosen as a reference against which to compare subsequent increasingly anisotropic examples. The selected impulse response is from the Arago cupola at the Paris Observatory, a late 19th century metallic semi-circular dome approximately 12 m in diameter with wooden floors and a large cast-iron telescope in the center.

A second enclosed space is also presented, as it was found to produce a noticeable degree of anisotropy: the main hall at the Lille opera house, an Italian-style 1136-seat layout with a $\sim$15$\times$18 m orchestra level and 4 highly vertical balcony rings (with very little overhang onto the orchestra level). Note that the stage was closed off by a metal curtain but the orchestra pit was open.

3.2 Semi-Open Space

Two DRIRs measured from within the 20$\times$23 m cloister garden at the former Dominican convent in Guebwiller, France, are used as examples where extreme anisotropy is expected since the space is open to the sky (i.e. free-field conditions toward the zenith from the SMA's point of view). Reverberation in the surrounding 3 m-wide partially-enclosed walkway is directly excited by the loudspeaker, but the garden wherein the receiver is placed has no roof and the ground is grass-covered.

3.3 Coupled Volumes

Finally, two coupled-volume configurations are compared in order to probe the direction-dependent characteristics of

such spaces as well as any possible relation to the emergence of double-sloped decays. The measurements, made respectively at the Christuskirche in Karlsruhe, Germany, and the modern Notre-Dame cathedral in Créteil, France, both involve the source and receiver being placed within small side chapels coupled to large, dome-like naves.

4. RESULTS

The spatial analysis framework presented above (Sec. 2) provides estimations of the direct sound's DoA, the mixing time t_{mix}, and the direction-dependent energy decay parameters (T_{60} reverberation time and P_0 initial reverberation power spectrum). Note that in this work the analysis framework was forced to use the directional steered PWD method regardless of the DRIR's degree of anisotropy in order to allow comparisons between the different results.

For each example, we present five figures chosen to give an overview of the analysis results. First, the spatial incoherence curve is displayed over the length of the denoised DRIR with t_{mix} and a frequency-averaged omnidirectional $\bar{t}_{\text{lim}}$ both highlighted. Next, the EDD of the denoised DRIR is projected onto both the azimuthal ($-180° < \theta \leq 180°$) and elevational ($-90° \leq \varphi \leq 90°$) planes (at fixed $\varphi = 0°$ and $\theta = 0°$, respectively) through spherical cubic Hermite interpolation [16]. Finally, 3D views of broadband averages of the two decay envelope parameters, the initial power P_0 and the reverberation time T_{60}, are shown. Both are interpolated from the 25 PWD steering directions onto a refined viewing grid (once more by spherical cubic Hermite interpolation [16]) and include the direct sound's DoA for reference. The spherical plots are shown from a viewing angle $(\theta_v, \varphi_v) = (45°, 22.5°)$, where $(\theta_0, \varphi_0) = (0°, 0°)$ corresponds to the x-axis and θ increases clockwise (negative left, positive right).

4.1 Enclosed Spaces

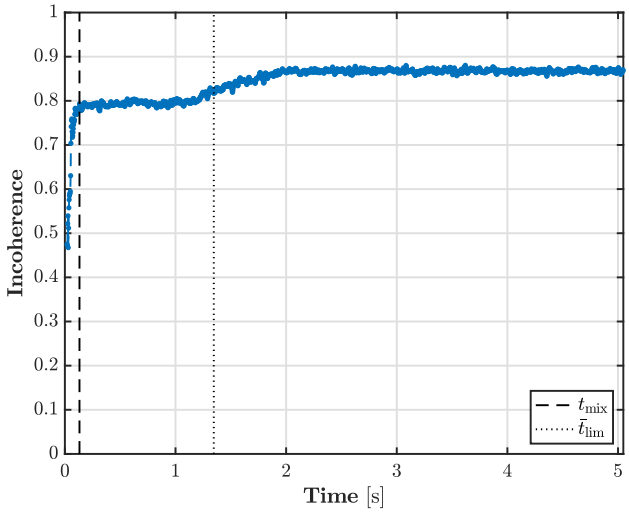

Figure 2. Arago cupola spatial incoherence profile, showing the mixing time (t_{mix}, dashed line) and average noise floor limiting time ($\bar{t}_{\text{lim}}$, dotted line).

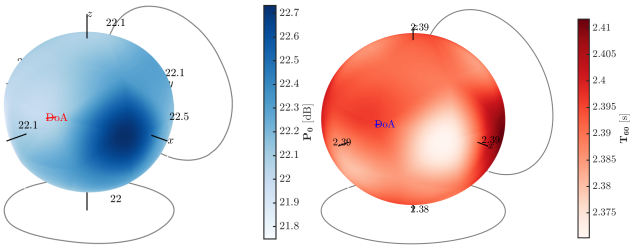

Figure 3. Arago cupola initial power P_0 (left) and T_{60} reverberation time (right). Direct sound DoA $\simeq (67°, 17°)$.

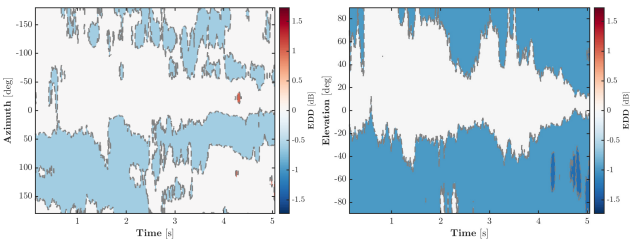

Figure 4. Arago cupola azimuthal and elevational plane EDDs (at $\varphi = 0°$ and $\theta = 0°$, respectively).

As mentioned in Sec. 3, the Arago cupola that sits atop the Paris observatory produces highly isotropic late reverberation with a clear single exponential decay. A high maximum spatial incoherence segment quickly reached for an estimated t_{mix} of 135 ms (Fig. 2). Note the increase in spatial incoherence around $\bar{t}_{\text{lim}}$ due to denoising by tail re-synthesis, which results in a slightly more incoherent field since the procedure currently re-synthesizes across all frequencies (thereby invalidating the low Schroeder frequency condition as well as removing any SMA high-frequency spatial aliasing).

The high isotropy is reflected in the very low spatial range and variation in both P_0 and T_{60} (Fig. 3): P_0 varies by less than 1 dB overall and T_{60} by less than 0.05 s. This isotropy is also reflected in a low EDD throughout the late reverberation tail (Fig. 4), which also mostly varies by less than 1 dB (exceptions appear at low elevations late in the reverberation tail, where the signal approaches the quantization noise floor and is thus subject to fluctuations due to numerical errors). Note that EDD figures are centered on zero, shown in white, indicating no energy deviation from the mean (a perfectly isotropic tail would thus be completely white). Darker colours indicate greater deviations from the mean (red for positive deviations, i.e. greater energy, and conversely blue for less energy and thus a negative deviation). Contours are drawn at steps of 1 dB.

The DRIR measured in the main hall of the Lille opera house shows that enclosed spaces can, in contrast to the above example, produce highly anisotropic decays. This DRIR also quickly reaches high incoherence (Fig. 5) for an estimated t_{mix} of 191 ms. The strong presence of coherent early reflections can be observed in the initial fluctuations of the incoherence profile ahead of the estimated mixing time. The anisotropic quality of the late reverberation is apparent in the range of over 6 dB of spatial P_0 vari-

ation (Fig. 6), although the T_{60} remains relatively isotropic (range of spatial variation around 0.08 s).

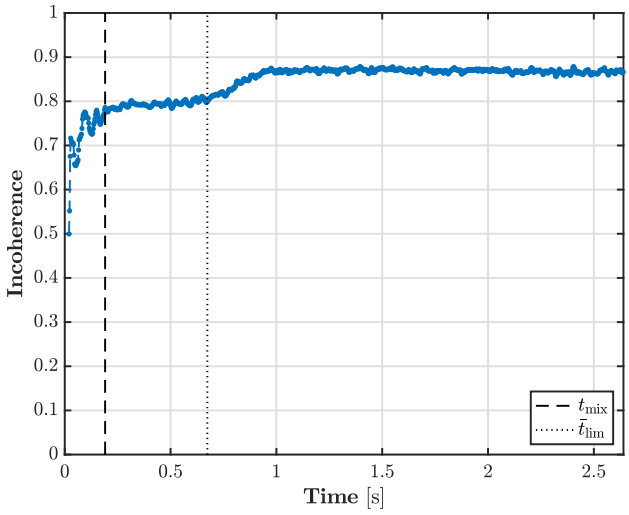

Figure 5. Lille opera house spatial incoherence profile, showing the mixing time (t_{mix}, dashed line) and average noise floor limiting time ($\bar{t}_{\mathrm{lim}}$, dotted line).

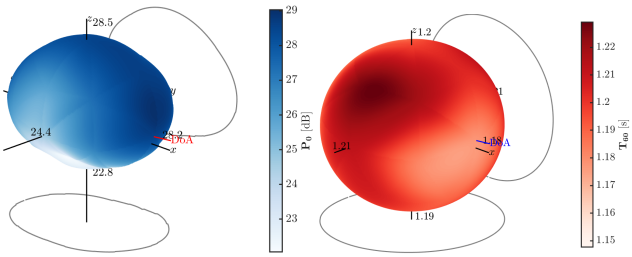

Figure 6. Lille opera house initial power P_0 (left) and T_{60} reverberation time (right). Direct sound DoA $\simeq (-1°, 5°)$.

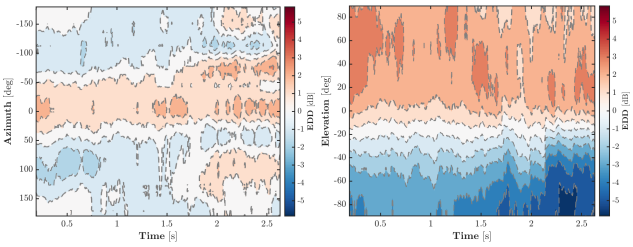

Figure 7. Lille opera house azimuthal and elevational plane EDDs (at $\varphi = 0°$ and $\theta = 0°$, respectively).

The EDD figures (Fig. 7) confirm that this anisotropy is mostly elevational (over 5 dB of deviation from the mean); although it is difficult to identify any exact causes, an uneven distribution of the room's absorptive and diffusive characteristics is likely a contributing factor. Since this measurement was taken with both source and receiver at the orchestra level, this could be seen to show that the cavity overhead resonates more than the plush seats below. In any case, these results seem to provide an insight into the space's acoustic properties.

4.2 Semi-Open Space

The following example confirms that the spatial analysis framework presented above enables the identification and modeling of highly anisotropic DRIRs. As mentioned above, the cloister at the Dominicains de Haute-Alsace convent is open to the sky, thus presenting free-field conditions above a certain elevation, and the only source of reverberation is the partially-enclosed walkway that surrounds the inner garden. The SMA was placed in the center of the 20×23 m garden. Two DRIRs are compared, taken with the loudspeaker placed successively in the centre of two perpendicular portions of the walkway, first facing the SMA along its x-axis, and second facing its y-axis. The spatial incoherence profile is shown for the x-axis DRIR in Fig. 8 with an estimated t_{mix} of 148 ms; the y-axis measurement gives a comparable estimate of 145 ms.

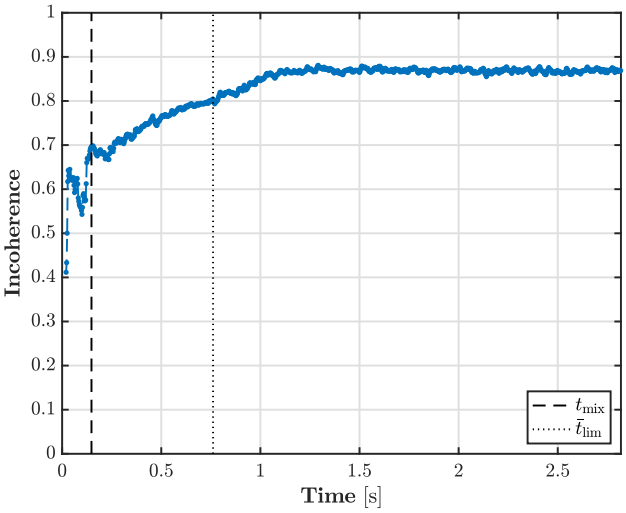

Figure 8. Convent cloister spatial incoherence profile (x-axis DRIR) showing the mixing time (t_{mix}, dashed line) and average noise floor limiting time ($\bar{t}_{\mathrm{lim}}$, dotted line).

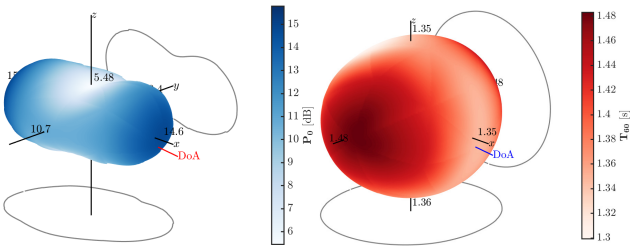

Figure 9. Convent cloister initial power P_0 (left) and T_{60} reverberation time (right, x-axis DRIR). Direct sound DoA $\simeq (-4°, -8°)$.

The decay envelope parameters (Fig. 9) display the highly anisotropic nature of this reverberation, with over 10 dB of spatial P_0 variation and an initial power that seems concentrated around the x-axis, which concords with the open sky above and the high absorptive grassy ground below. Although the T_{60} only varies by around 0.18 s, it does appear to show some geometric characteristics as well, being longer along the y-axis than any other.

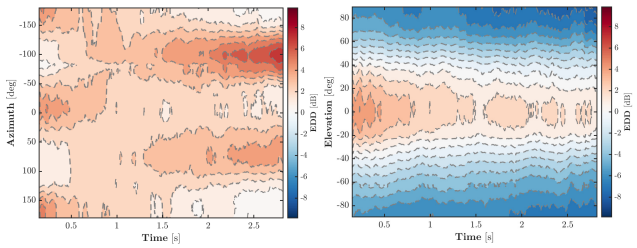

Figure 10. Convent cloister azimuthal and elevational plane EDDs (at $\varphi = 0°$ and $\theta = 0°$, respectively), x-axis DRIR (direct sound DoA $\simeq [-4°, -8°]$).

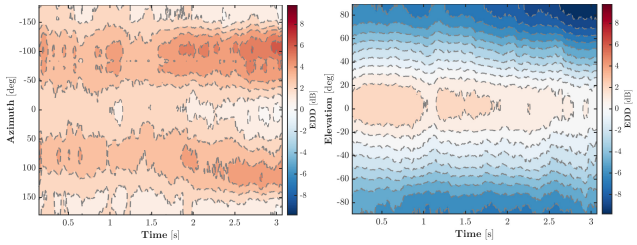

Figure 11. Convent cloister azimuthal and elevational plane EDDs (at $\varphi = 0°$ and $\theta = 0°$, respectively), y-axis DRIR (direct sound DoA $\simeq [80°, 2°]$).

However, the highly directional nature of this DRIR and the complex nature of the space requires any interpretation of these results to take into account the influence of the loudspeaker's directivity, and more specifically any deviation from perfect omnidirectionality.

It is therefore useful to compare the results from both the x and y-axis measurements in order to gain a better understanding of which characteristics are "true" to the space and which were further due to directional excitation of the loudspeaker. The EDD figures (Fig. 10 for the x-axis DRIR and Fig. 11 for the y-axis) show that, as could be expected, the elevational characteristics remain the same (the reverberation is almost exclusively lateral), but the two measurements differ on the azimuthal plane. It appears that whereas the x-axis measurement excited "early" late reverberation along the x-axis ($\theta = 0°$ and $\theta = \pm 180°$) before settling along the y-axis ($\theta = \pm 90°$) (in accordance with the decay parameters, Fig. 9), the y-axis measurement remains entirely concentrated along the y-axis. This suggests that the space's reverberation does have a natural tendency to settle on the y-axis, although a non-omnidirectional loudspeaker may excite the space differently from different directions. It should also be noted here that the mixing time is estimated at a comparitavely low incoherence value (Fig. 8), suggesting the presence of coherent early reflections during the early part of the late reverberation tail, which may be a contributing factor in the differences observed between the two measurements.

4.3 Coupled Volumes

The final examples presented here are two DRIRs measured in similar coupled-volume configurations (both small annex chapels giving onto large dome-shaped naves)

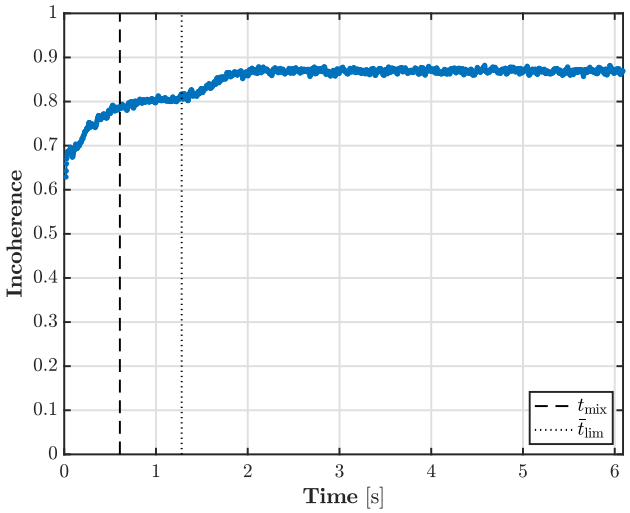

Figure 12. Christuskirche coupled chapel spatial incoherence profile, showing the mixing time (t_{mix}, dashed line) and average noise floor limiting time ($\bar{t}_{\mathrm{lim}}$, dotted line).

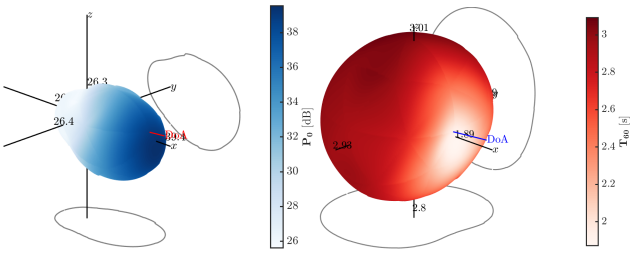

Figure 13. Christuskirche coupled chapel initial power P_0 (left) and T_{60} reverberation time (right). Direct sound DoA $\simeq (4°, 7°)$.

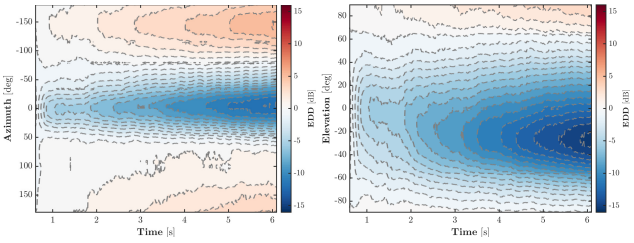

Figure 14. Christuskirche chapel azimuthal and elevational plane EDDs (at $\varphi = 0°$ and $\theta = 0°$, respectively).

that yield notably different spatial analysis results. In particular, the Christuskirche measurement seems to lack the double-sloped decay characteristic of coupled-volume acoustics (when both source and receiver are placed within the less reverberant space) [23], whereas the Créteil cathedral DRIR does indeed present this property. The spatial incoherence profile for the Christuskirche (Fig. 12), from which a comparatively long t_{mix} of 607 ms is estimated, seems to suggest that perhaps only a single slope is detected because the initial rapid decay is not incoherent enough to be considered late reverberation. Indeed, the mixing time appears to correspond to the onset of the second slope, an interpretation corroborated by the EDD (Fig. 14), which begins at t_{mix} by definition and shows

only a single directional tendency.

However, another interpretation would suggest that the two slopes are highly separated direction-wise, and can thus be treated as different single slopes in different directions. This view is brought to light by the decay envelope parameters (Fig. 13), which show that near the estimated direct sound DoA of $(3.7°, 6.8°)$ the late reverberation reaches both a maximum initial power of 39.5 dB and a minimum T_{60} of 1.87 s while in the opposite direction (toward the coupled volume) it conversely presents a minimum P_0 of 25.6 dB and a maximum T_{60} of 3.09 s.

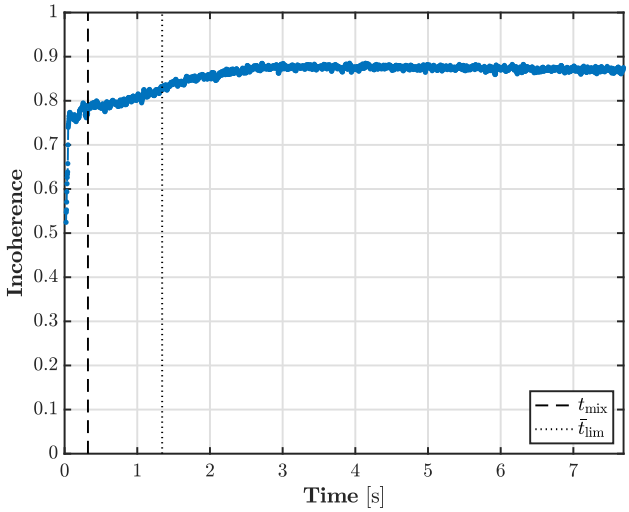

Figure 15. Créteil cathedral chapel spatial incoherence profile, showing the mixing time (t_{mix}, dashed line) and average noise floor limiting time ($\bar{t}_{\mathrm{lim}}$, dotted line).

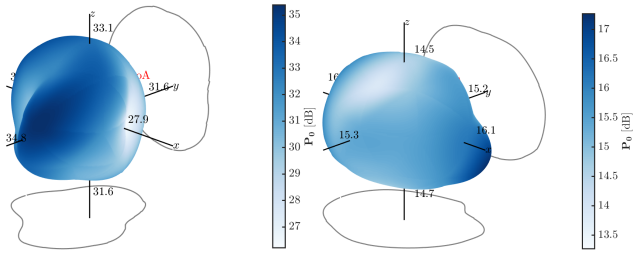

Figure 16. Créteil cathedral coupled chapel initial power P_0; first slope (left) and second slope (right). Direct sound DoA $\simeq (-116°, 0°)$.

On the other hand, a double-slope decay is readily detected in the Créteil cathedral DRIR. This space appears to mix much more readily than the Christuskirche example, with a high level of incoherence quickly reached (Fig. 15) for an estimated t_{mix} of 321 ms. Although the directional P_0 for the two slopes (Fig. 17) follows a similar logic to that of the Christuskirche, with the first (left) stronger towards the smaller volume containing both source and receiver and the second (right) towards the coupled highly reverberant space, the directional separation is far less extreme. Additionally, the reverberation times are far more isotropic, with spatial variation ranges of only 0.57 s and 0.40 s for the two slopes, respectively.

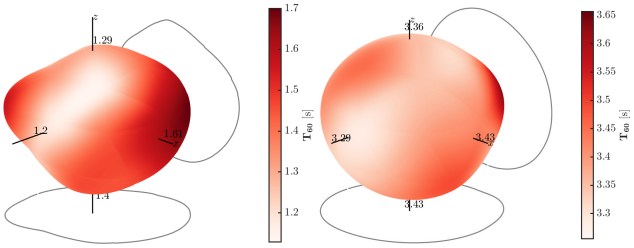

Figure 17. Créteil cathedral coupled chapel T_{60} reverberation time; first slope (left) and second slope (right). Direct sound DoA $\simeq (-116°, 0°)$.

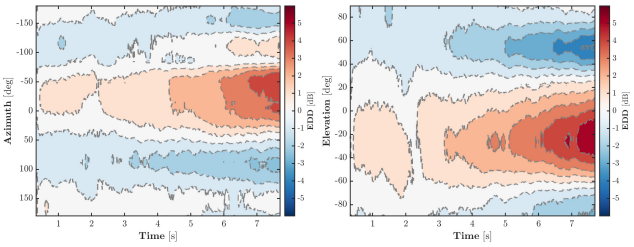

Figure 18. Créteil cathedral chapel azimuthal and elevational plane EDDs (at $\varphi = 0°$ and $\theta = 0°$, respectively).

The lack of a clear directional separation between the two slopes does not make the late reverberation entirely isotropic, however. As evidenced by the EDD figures (Fig. 18), the anisotropy of the second slope especially leads to a strong directional tendency throughout the late reverberation tail (in the direction of the reverberating coupled nave toward which the Eigenmike was facing).

5. CONCLUSION

This paper has presented and discussed results obtained through the application of a comprehensive spatial analysis framework for late reverberation to a range of DRIRs measured using an mh acoustics Eigenmike SMA. These DRIRs cover a wide variety of acoustic spaces and each display particular late reverberation characteristics that can be brought to light using the analysis tools described in Sec. 2. Specifically, the framework relies on spatial incoherence analysis, which enables mixing time estimation, directional decay envelope modeling, from which the initial reverberation power P_0 and the 60 dB reverberation time T_{60} can be determined, and finally a measure of the DRIR's directional energy distribution throughout the late reverberation tail using the EDD.

The results presented in Sec. 4 show that these analysis techniques can provide significant insights into the spatial properties of a space's late reverberation. Furthermore, they confirm that the directional denoising procedure first introduced in Massé *et al.* [8] preserves these spatial properties throughout its prolongation of the reverberation tail.

Several aspects of the work presented in this paper merit further research. First and foremost, and although not discussed here due to being beyond the scope of this particular paper, the use of a discretized and order-truncated PWD

imposes several limitations on the accuracy of the directional decay envelope analysis. As such, several alternatives are currently being pursued in order to improve the spatial decomposition of the late reverberation tail through a dedicated spatial filter bank formalism. Secondly, in the interest of developing a complete toolset for manipulating DRIRs, methods for detecting and treating the discrete early reflections are also under investigation. Finally, in order to provide more intuitive control over these manipulations, it would be necessary to link the DRIR analysis framework to perceptual descriptors such as listener envelopment (LEV) or apparent source width (ASW) [24].

6. REFERENCES

[1] J.-M. Jot, L. Cerveau, and O. Warusfel, "Analysis and Synthesis of Room Reverberation Based on a Statistical Time-Frequency Model," in *Proc. 103rd A.E.S. Conv.*, (New York, U.S.A.), 1997.

[2] M. R. Schroeder, "Natural-Sounding Artificial Reverberation," *J.A.E.S.*, vol. 10, no. 3, pp. 219–223, 1962.

[3] J. A. Moorer, "About This Reverberation Business," *Computer Music Journal*, vol. 3, no. 2, pp. 13–28, 1979.

[4] J.-D. Polack, *La transmission de l'énergie sonore dans les salles*. PhD thesis, Université du Maine, 1988.

[5] T. Carpentier, T. Szpruch, M. Noisternig, and O. Warusfel, "Parametric Control of Convolution-Based Room Simulators," in *Proc. 2013 I.S.R.A.*, (Toronto, Canada), 2013.

[6] M. Noisternig, T. Carpentier, T. Szpruch, and O. Warusfel, "Denoising of Directional Room Impulse Responses Measured with Spherical Microphone Arrays," in *Proc. 40th DAGA*, (Oldenburg, Germany), pp. 600–601, 2014.

[7] P. Massé, T. Carpentier, O. Warusfel, and M. Noisternig, "A Robust Denoising Process for Spatial Room Impulse Responses with Diffuse Reverberation Tails," *J.A.S.A.*, vol. 147, no. 4, pp. 2250–2260, 2020.

[8] P. Massé, T. Carpentier, O. Warusfel, and M. Noisternig, "Denoising Directional Room Impulse Responses with Spatially Anisotropic Late Reverberation Tails," *Applied Sciences*, vol. 10, no. 3, p. 1033, 2020.

[9] D. Romblom, C. Guastavino, and P. Depalle, "Perceptual Thresholds for Non-Ideal Diffuse Field Reverberation," *J.A.S.A.*, vol. 140, no. 5, pp. 3908–3916, 2016.

[10] M. Berzborn and M. Vorländer, "Investigations on the Directional Energy Decay Curves in Reverberation Rooms," in *Proc. 11th Euronoise*, 2018.

[11] B. Alary, P. Massé, V. Välimäki, and M. Noisternig, "Assessing the Anisotropic Features of Spatial Impulse Responses," in *Proc. EAA S.A.S.P. Symp.*, (Paris, France), pp. 43–48, 2019.

[12] M. Nolan, E. Fernandez-Grande, J. Brunskog, and C.-H. Jeong, "A Wavenumber Approach to Quantifying the Isotropy of the Sound Field in Reverberant Spaces," *J.A.S.A.*, vol. 143, no. 4, pp. 2514–2526, 2018.

[13] J. Ahonen and V. Pulkki, "Diffuseness Estimation Using Temporal Variation of Intensity Vectors," in *Proc. 2009 IEEE W.A.S.P.A.A.*, (New Paltz, U.S.A.), pp. 285–288, IEEE, 2009.

[14] J. Fliege and U. Maier, "A Two-Stage Approach for Computing Cubature Formulae for the Sphere," *Mathematik 139T, Universitat Dortmund, Fachbereich Mathematik, Universitat Dortmund, 44221*, pp. 1–31, 1996.

[15] N. Epain and C. T. Jin, "Spherical Harmonic Signal Covariance and Sound Field Diffuseness," *IEEE/ACM T.A.S.L.P.*, vol. 24, no. 10, pp. 1796–1807, 2016.

[16] C. L. Lawson, "C1 Surface Interpolation for Scattered Data on a Sphere," *Rocky Mountain Journal of Mathematics*, vol. 14, no. 1, pp. 177–202, 1984.

[17] J. Merimaa and V. Pulkki, "Spatial Impulse Response Rendering I: Analysis and Synthesis," *J.A.E.S.*, vol. 53, no. 12, pp. 1115–1127, 2005.

[18] B. Jo, F. Zotter, and J.-W. Choi, "Extended Vector-Based EB-ESPRIT Method," *IEEE/ACM T.A.S.L.P.*, 2020.

[19] H. Kuttruff, *Room Acoustics*. London, U.K.: Spon Press, fourth ed., 2000.

[20] D. K. Prasad, M. K. Leung, C. Quek, and S. Y. Cho, "A Novel Framework for Making Dominant Point Detection Methods Non-Parametric," *Image and Vision Computing*, vol. 30, no. 12, pp. 843–859, 2012.

[21] J. Daniel and S. Moreau, "Further Study of Sound Field Coding with Higher Order Ambisonics," in *Proc. 116th A.E.S. Conv.*, (Berlin, Germany), 2004.

[22] B. Rafaely, "Analysis and Design of Spherical Microphone Arrays," *IEEE T.A.S.L.P.*, vol. 13, no. 1, pp. 135–143, 2005.

[23] L. Cremer, H. A. Müller, and T. J. Schultz, *Principles and Applications of Room Acoustics, vol. 1*. Barking, England: Applied Science Publishers, 1982.

[24] D. Griesinger, "Objective Measures of Spaciousness and Envelopment," in *Proc. A.E.S. 16th Int. Conf. on Spatial Sound Reproduction*, pp. 1–15, 1999.